Check for updates

Received: 13 February 2021 | Revised: 6 July 2021 | Accepted: 9 August 2021

DOI: 10.1002/ppp.2131

RESEARCH ARTICLE

WILEY

Effects of a long-term anoxic warming scenario on microbial community structure and functional potential of permafrost-affected soil

Sizhong Yang[1,2] | Susanne Liebner[1,3] | Josefine Walz[4] | Christian Knoblauch[4,5] | Till L. V. Bornemann[6] | Alexander J. Probst[6] | Dirk Wagner[1,7] | Mike S. M. Jetten[8,9] | Michiel H. in 't Zandt[8,10]

[1]GFZ German Research Centre for Geosciences, Section Geomicrobiology, Telegrafenberg, Potsdam, Germany

[2]Cyrosphere Research Station on the Qinghai-Tibet Plateau, State Key Laboratory of Cryospheric Sciences, Northwest Institute of Eco-Environment and Resources, Chinese Academy of Sciences, Lanzhou, China

[3]Institute of Biochemistry and Biology, University of Potsdam, Potsdam, Germany

[4]Institute of Soil Sciences, Department of Earth System Sciences, Universität Hamburg, Hamburg, Germany

[5]Center for Earth System Research and Sustainability, Universität Hamburg, Hamburg, Germany

[6]Environmental Microbiology and Biotechnology, Faculty of Chemistry, University of Duisburg-Essen, Essen, Germany

[7]Institute of Geosciences, University of Potsdam, Potsdam, Germany

[8]Department of Microbiology, Institute for Water and Wetland Research, Nijmegen, AJ, The Netherlands

[9]Soehngen Institute of Anaerobic Microbiology, Radboud University, Nijmegen, AJ, The Netherlands

[10]Netherlands Earth System Science Center, Utrecht University, Utrecht, CS, The Netherlands

Correspondence
Sizhong Yang, GFZ German Research Centre for Geosciences, Section Geomicrobiology, Telegrafenberg, 14473 Potsdam, Germany.
Email: syang@gfz-potsdam.de

Present address
Josefine Walz, Climate Impacts Research Centre, Department for Ecology and Environmental Science, Umeå University, Abisko, Sweden

Michiel H. in 't Zandt, KWR Water Research Institute, Nijmegen, Gelderland, Netherlands

Abstract

Permafrost (PF)-affected soils are widespread in the Arctic and store about half the global soil organic carbon. This large carbon pool becomes vulnerable to microbial decomposition through PF warming and deepening of the seasonal thaw layer (active layer [AL]). Here we combined greenhouse gas (GHG) production rate measurements with a metagenome-based assessment of the microbial taxonomic and metabolic potential before and after 5 years of incubation under anoxic conditions at a constant temperature of 4°C in the AL, PF transition layer, and intact PF. Warming led to a rapid initial release of CO_2 and, to a lesser extent, CH_4 in all layers. After the initial pulse, especially in CO_2 production, GHG production rates declined and conditions became more methanogenic. Functional gene-based analyses indicated a decrease in carbon- and nitrogen-cycling genes and a community shift to the degradation of less-labile organic matter. This study reveals low but continuous GHG production in long-term warming scenarios, which coincides with a decrease in the relative abundance of major metabolic pathway genes and an increase in carbohydrate-active enzyme classes.

KEYWORDS
climate change, greenhouse gases, microbial dynamics, permafrost

This is an open access article under the terms of the Creative Commons Attribution License, which permits use, distribution and reproduction in any medium, provided the original work is properly cited.
© 2021 Helmholtz-Zentrum Potsdam - Deutsches GeoForschungsZentrum (GFZ). *Permafrost and Periglacial Processes* published by John Wiley & Sons Ltd.

Funding information
German Ministry of Education and Research, Grant/Award Numbers: CarboPerm (03G0836A, 03G0836D), KoPf (03F0764A, 03F0764F); Helmholtz-Gemeinschaft, Grant/Award Number: VH-NG-919 to Susanne Liebner; National Key Research and Development Program of China, Grant/Award Number: 2020YFA0608501; Chinese Academy of Sciences; German Research Foundation (DFG); European Research Council Advanced Grant, Grant/Award Number: 339880 to Mike Jetten; Soehngen Institute of Anaerobic Microbiology (SIAM) Gravitation Grant, Grant/Award Number: 024.002.002; Netherlands Organization for Scientific Research, Netherlands Earth System Science Center (NESSC), Grant/Award Number: 024.002.001; Ministry of Culture and Science of NorthRhine-Westphalia (Nachwuchsgruppe "Dr. Alexander Probst")

1 | INTRODUCTION

Permafrost (PF), which is classified as ground that stays frozen for at least two consecutive years, is widespread in the Arctic and subarctic regions. PF -affected soils in these regions store ~1,300 Pg carbon, which equals 50% of the global belowground organic carbon, and the major fraction (~1,000 Pg) is stored in the upper 3 m of soil.[1] Over the past 30 years, high-latitude areas have warmed at a rate of 0.6°C per decade, which is twice as fast as the global average.[2] Modeled extremes predict a temperature increase of up to 7–8°C by the end of this century.[3] Consequently, the thawing of PF exposes large organic carbon stocks to decomposition by soil microorganisms.[4] This in turn could release the sequestered frozen long-term carbon stocks into the atmosphere as greenhouse gases (GHGs), carbon dioxide (CO_2) and methane (CH_4).[5,6] Although recent data on carbon isotopes imply that CH_4 derived from older carbon substrates is released relatively slowly, the increasing decomposition of PF carbon leads to a net positive contribution to the global atmospheric GHG budget.[7] This release initiates a positive climate feedback loop.[8–11]

The active layer (AL) of PF-affected soils is exposed to seasonal freeze–thaw cycles, whereas the underlying PF is characterized by year-round below-zero temperatures and low water availability. The uppermost part of the PF, which is called the transition layer (TL), is more prone to thaw than deeper PF. This layer differs in cryo-features, carbon, and moisture content from the underlying PF and is irregularly exposed to thaw.[4,12] During thaw, water accumulation can lead to rapid gas diffusion limitation and a subsequent depletion of oxygen in the deep AL, whereas drainage of melted water allows oxygen penetration into deeper soils. Thus, hydrology plays an important role in regulating the soil redox potential and therefore the conditions for aerobic and anaerobic microbial metabolism.[13] In particular, anaerobic microbial carbon turnover processes remain poorly understood.[6] In addition, changes in soil temperature, nutrient availability, and vegetation influence soil organic carbon (SOC) decomposition and the resulting ratio of CO_2 to CH_4 emissions.[13–15] The SOC quality is important to influence carbon release from PF; however, a labile carbon pool is usually degraded immediately after PF thawing, and slow decomposing carbon fraction determines the long-term decomposition of PF SOC on a scale of 5–15 years.[16] After the initial degradation of labile organic matter fractions, microbes have access to less-labile organic matter fractions. These organic compounds are mainly degraded by microbial guilds with cellulase and hemicellulase activity.[16,17] Therefore, the microbial community is expected to shift toward a population that degrades less-labile organic matter in the long term.

Increasing global efforts have recognized the need to understand the microbial ecology of thawing PF to better predict its role and fate in a warmer world, especially its impact on the global carbon budget.[10,18] Repeated freeze–thaw cycles modify the AL communities to conserve energy and obtain nutrients from a diversity of substrates through aerobic and anaerobic processes as well as adapt to survival under dynamic freeze–thaw conditions.[19] In contrast, microbial communities in PF layers can be very well conserved and of ancient origin.[19–22] In extreme cryogenic environments, the microbial community is likely to maintain a high level of stress tolerance due to long-term cold exposure.[18,23] PF thawing leads to shifts in microbial diversity, abundance, and activity within days to months.[20,24,25] Short-term thaw exposure (2–7 days) can cause a change in gene composition of former PF communities to resemble the AL.[20] These findings suggest that prolonged exposure to thaw will likely lead to even stronger shifts in community structures. The taxonomic and functional shifts, especially the enrichment of genes involved in the carbon and nitrogen cycle as well as respiratory processes, were identified from short-term thaw experiments and field studies on PF thawing.[20,26–28] Microbiota in a PF-affected peatland can modulate the metabolic and trophic interactions to maintain high fermentation rates and CH_4 production.[26] In addition, dominant processes shaping microbial communities in PF resulted from the stability of the PF environment, which imposed both dispersal and thermodynamic constraints.[29] This suggests pronounced differences in the microbial metabolic potential between the AL and PF soils.

Comparative studies on AL versus PF microbial communities, are, however, scarce,[20,30] and most previous studies focused on either AL[31–34] or PF microbial communities.[29,35,36] It is obvious that integrally studying these layers is important, because the deepening of the AL results in cryoturbation on the interannual scale in the PF -AL transition zone.[12] This can serve as a selective pressure on the PF microbial communities that are progressively exposed within the transient layer. The microbial community also has to adjust to a decrease in carbon availability as less-labile carbon fractions are left after easy-degradable fractions are depleted within a few years after PF thaw.[37] The pool of previously frozen SOC is largely responsible for sustained carbon loss in thermokarst-active PF regions. However, the long-term consequences of PF thaw to the microbial community composition and potential are not well understood.[13,18]

Understanding the microbial dynamics on PF soil thaw and warming beyond timescales of days and weeks is important to improve current predictive climate models for cold environments and to refine our knowledge of the magnitude and timing of PF carbon emissions in a warming world. Incubation experiments, even if artificial, are commonly used to inform valuable parameters for process-based modeling of the PF carbon feedback.[6,16,26,38,39] In particular, models expect a robust response under boundary conditions to help reduce uncertainty and provide a better estimate of impacts under different scenarios (e.g., references 6 and 40). In contrast to fast labile carbon that represents less than 5% of SOC at long turnover time (5–15 years),[16] the previously frozen old carbon dominates the carbon release from the northern PF regions where thermokarst landscape is extensively developed.[41] For this reason, the investigation of microbial decomposition on old carbon on climate-relevant timescales to the maximum potential can provide valuable reference for modeling study. Therefore, we conducted a long-term incubation without additional nutrient amendment to explore the response capability of microbial system at lower boundary conditions. On thaw and long-term warming of PF soils under anoxic conditions, we hypothesize that the microbial communities adapt to the depletion of available carbon and alternative terminal electron acceptors, through taxonomic and functional shifts, in spite of the heterogeneity of initial geochemistry and the microbial community between the AL and PF. A lab-scale incubation experiment was performed at 4°C for more than 5 years under anoxic conditions. Full metagenomic sequencing at the start and end of the incubation was coupled to measurements of geochemistry as well as CO_2 and CH_4 production rates. The results can provide insights into the effects of batch incubation conditions on GHG production for future modeling studies.

2 | MATERIALS AND METHODS

2.1 | Study site and sampling

The study site is located at Samoylov Island (72°22′N, 126°30′E), in the Lena River delta in Northeast Siberia, Russia. Samoylov Island developed during the Holocene and is underlain by continuous PF. The mean annual air temperature is −12.5°C (1998–2011), the mean annual precipitation is 125 mm, and the mean soil temperatures (MST) is 4.1°C at a depth of 20 cm in the warmest month of August (mean air temperature 8.5°C in August).[42] On the island, ice-wedge polygons are extensively developed with low-lying polygon centers and elevated polygon rims on the surface. The dominating vascular plant species in the polygon centers is the sedge *Carex aquatilis*.[43,44] Samples were taken from a polygon center in spring 2011 when the soil was entirely frozen. The location and sampling procedures of the polygon used for this study are described earlier.[45] According to our previous study, oxygen depleted in the upper centimeters due to waterlogging.[46] Limited by remoteness, logistics, and harsh cold sampling season, the samples retrieved from the field in the frozen season are scarce, therefore limiting the use in multiple experiments and replication studies. In this study, the samples from the AL (15–22 cm), TL (33–37 cm), and PF (42–51 cm) were used for incubations. For this study, we performed GHG flux analyses (three biological replicates for GHG production), chemical analysis (two technical replicates), and a time series of molecular analyses (three samples for each time point) to follow the general trend of microbial response to long-term warming exposure of the three distinct zones of a thaw-affected PF soil. Here we report the results of the first time point (5 years) after incubation.

2.2 | Pore water and bulk soil analysis

All initial samples were analyzed for pore water chemical composition and bulk element content. Major cations (NH_4^+, Ca^{2+}, K^+, Mg^{2+}, and Na^+) and anions (Cl^-, NO_3^-, NO_2^-, and SO_4^{2-}) in pore water of the initial samples were analyzed by using nonsuppressed and suppressed ion chromatography (Sykam, Fürstenfeldbruck, Germany). Ferric [Fe(III)] and ferrous [Fe(II)] iron were measured using spectrophotometry (DR3900, Hach Lange GmbH, Düsseldorf, Germany) according to the ferrozine method.[47] The measurements were conducted in an anaerobic glove box to inhibit the oxidation of Fe(II). In addition, bulk soil samples were dried at 70°C and milled for measuring the total carbon and nitrogen content (Vario MAX cube, Elementar GmbH, Langenselbold, Germany). Soil water contents were calculated as the weight difference between wet and dried (105°C) samples. pH values were measured in a suspension of 5 g of thawed soil in 12.5 mL of distilled water (CG820, Schott Geräte GmbH, Hofheim, Germany).

2.3 | Anoxic incubations

Samples from AL, TL, and PF were incubated in the dark at 4°C under anoxic conditions for more than 5 years. Here, the selected incubation temperature was the MST of 4.1°C at a depth of 20 cm in warm August[42] under oxygen-depleted conditions, which are common in this area.[46] No nutrient amendment mimicked the boundary response and minimized additional biases. During the incubation, GHG production was followed for 1,163 days.[6,45] As the CH_4 production rates remained fairly constant and low in the long term, production rate measurements

were stopped after 1,163 days, but the incubations were maintained as mentioned earlier. The anoxic incubations were prepared under a N_2 atmosphere in a glove box. Briefly, samples were thawed and equilibrated in a refrigerator at ~2°C for 1 day. Approximately 20 g of thawed soil was weighed in glass bottles and sealed with butyl-rubber stoppers. Each bottle was amended with 10 mL of N_2-flushed, O_2-free demineralized water, and the headspace was thoroughly exchanged with molecular nitrogen for 30 min. Subsequently, CO_2 and CH_4 concentrations were measured repeatedly, with a maximum time interval of 140 days. GHG production rates were calculated by a moving window for every four measurements ($\mu g\ d^{-1}\ gSOC^{-1}$).

2.4 | DNA extraction, qPCR, and sequencing

DNA was extracted from both pre-incubation and post-incubation samples. The original (pre-incubation) samples were preserved at −80°C until further DNA extraction. Before DNA extraction, plant residues were removed step by step using sterilized sieves (2, 1, and 0.5 mm) in slurries with 1× phosphate-buffered saline (PBS) under aseptic conditions. The PBS flow-through was pooled with the remaining material (after sieving), and the material was filtered through a 0.2-μm pore size filter. The total genomic DNA was extracted through the filter using the phenol–chloroform method.[26] After RNA was removed with RNaseA (0.5 μL, 10 mg mL^{-1} per reaction) at 4°C, the obtained DNA was sent for paired-end sequencing at GATC Biotech (now Eurofins Scientific, Constance, Germany), on an Illumina Hiseq 2500 system.

Quantitative polymerase chain reaction (qPCR) was conducted using a CFX Real-Time PCR Detection System (Bio-Rad Laboratories, CA, USA). The primer sets Eub341-F/Eub534-R and mlas/mcrA-rev were used to target bacteria and methanogenic archaea, respectively.[48] The reaction solutions contain iTaq Universal SYBR Green Supermix (Bio-Rad Laboratories), 0.5 μM primer each, and 2 μL of diluted (1:100) template DNA. The qPCR assays involve the following steps: initial denaturation for 3 min at 95°C, followed by 40 cycles of denaturation for 3 s at 95°C, annealing for 20 s at 58.5°C, elongation for 30 s at 72°C, and a plate read step at 80°C for 0.3 s. Melt curve analysis from 65 to 95°C with a 0.5°C temperature increment per 0.5-s cycle was conducted at the end of each run. Based on standard curves, the PCR efficiencies ranged between 93 and 99%.

Raw metagenomic sequences were processed with the ATLAS metagenomic pipeline (v2.0.6)[49] following the standard procedure. Briefly, the workflow includes quality control (QC), assembly (metaSPADes was used in this study), genome binning, and annotation (for details please refer to reference 49). In total, 89 Gb of metagenomic sequence data were generated (70.8–84.5 million raw sequences per sample, 97.84–98.36% sequences passed QC). The N50 ranges from 101 to 139 kb, and L50 ranges from 1,644 to 2,294 bp (refer to Table S1 for assembly summary statistic). The high-quality contigs were used for gene prediction using Prodigal,[50] and the translated gene products were functionally annotated by eggNOG-mapper (v1.0.3).[51] Furthermore, the translated protein sequences were taxonomically annotated using DIAMOND (v0.8.22.84)[52] by referring to UniRef90 (https://www.uniprot.org/).[53] The KEGG (Kyoto Encyclopedia of Genes and Genomes) (i.e., KO identifiers) and Clusters of Orthologous Genes (COG) annotations were obtained from the EggNOG reference database (v5.0).[54]

During downstream analysis, we reconstructed the relative abundances of the functional categories of methanogenesis, carbon fixation, nitrogen cycling, and sulfur cycling at whole community level. All related functional components were extracted according to the KO identifiers of major pathways from the KEGG database by using custom Python, R, and shell scripts. The gene abundances were normalized to transcripts per kilobase million (TPM) by considering both gene length and coverage. To identify the functional components of carbon degradation pathways, the subsets of the carbohydrate-active enzyme (CAZy) annotations were extracted from the output of eggNOG-mapper (v1.0.3). Subsequently, the abundance of each functional category was normalized to TPM within this CAZy subset. In addition, all the CAZy-affiliated protein sequences were taxonomically assigned against UniRef90 database[53] by using DIAMOND (v0.8.22.84) to identify the major microbial players.

To obtain an overall scenario of the taxonomic differentiation at community level, we also assigned taxonomic labels to the merged paired-end QC short reads by mapping against the SILVA 132 SSU nonredundant reference database[55] using local blast (v2.6.0+).[56] The taxonomy was reported maximally at family level due to the relatively short-sequence fragment lengths (which are 203, 243, and 269 bp at 25, 50, and 75% quantiles for the merged paired-end reads, respectively). Length and similarity fraction were set to 180 and 70%, respectively, resulting in 74,765 mapped merged paired-end reads. In addition, the taxonomic composition was assigned based on the annotated ribosomal protein S3 (rpS3, which was also recently proposed as "uS3" according to the Ban Lab, https://bangroup.ethz.ch/research/nomenclature-of-ribosomal-proteins.html). The rpS3 marker detects organisms with incomplete or unavailable SSU rRNA gene sequences and more strongly resolves the evolutionary deeper radiations.[57] Therefore, it was used as an alternative approach to analyze the general change in microbial community composition on warming. However, the reference database is less extensive for rpS3 than for the SSU rRNA, and the analysis is more sensitive to the quality of the assembly process than that of the SSU rRNA. Details of this analysis can be found in Supplementary Document 1.

Microbial community visualization was performed in R.[58] Community data were collapsed at higher taxonomic level with the R package otuSummary.[59] Ordination analyses of microbial community structure were performed with the R package vegan (v2.5-2).[60] Heatmaps were generated with the package ggplot2 (v3.1.0).[61] In addition, the fold changes incubated with respect to the initial relative abundance of taxonomic composition were used to semiquantitatively estimate the extent of abundance shifts for various microbial taxa. The fold changes were visualized via a bubble plot with ggplot2 (v3.1.0). Principal Coordinates Analysis (PCoA) and symmetric procrustes analysis on the functional and taxonomic profiles were performed by using Bray–Curtis dissimilarity with package vegan

(v2.5-2).[60] Permutational analysis of variance on the CH_4 production rates over layers was performed with the kruskal.test function in R.[58] In addition, permutation test was used to compare the changes in functional profile by layer in R.

2.5 | Data deposition

The data were deposited at EMBL-EBI under accession number ERS4594325-ERS4594330 (Bioproject PRJEB38557).

3 | RESULTS

3.1 | CO_2 and CH_4 production rates

The CO_2 and CH_4 production rates were monitored within the AL, TL, and PF layers over the course of 1,163 days to gain insights into GHG production rates under anoxic thaw conditions in the long term (Figure 1). The CO_2 production rates peaked during the first 50–100 days of incubation, and then a rapid decrease was observed for all layers. Then, CO_2 production rates were similar in the different layers, with slightly higher levels observed in AL. The initial CH_4 production rates were about an order of magnitude lower than CO_2 production rates. In AL the rates did not show a lag phase, and production rates peaked after ~ 200 days, after which a gradual decrease was observed. After ~750 days, a marginal increase was observed. The TL showed a slight initial peak associated with direct CH_4 release followed by a short lag phase of 50–75 days. The CH_4 production in TL was more stable, with a slight increase in production after ~ 600 days. The PF exhibited the smallest initial release of CH_4, followed by the longest lag phase between 20 and 150 days. The CH_4 production rates in PF were relatively constant, with lower peaks around 300 and 750 days. In PF, the highest CH_4 production rates were observed after more than 2 years of incubation. For detailed CH_4 production data, see Figure S1. Permutational test on the measured CH_4 production rate ($n = 43$) was statistically different between the three layers ($p < 0.01$). The ratio between the cumulative CO_2 and CH_4 production showed similar patterns in all the layers. All ratios were initially >8, and they approached 1 around 300 days of incubation, which indicates that the conditions became more methanogenic.

3.2 | Physicochemical pore water and bulk soil properties

Pore water analysis on initial samples indicated clear differences between AL, TL, and PF (Figure S2). Ammonium concentrations decreased along the depth gradient (2.0, 0.7, and 0.3 mg L^{-1}, respectively). Overall, nitrite was very low (<0.1 mg L^{-1}), and nitrate was negligible (<0.01 mg L^{-1}, not shown). Sulfate contents were highest in AL and TL (2.9 and 3.3 mg L^{-1}) and lowest in PF (1.5 mg L^{-1}). PF was

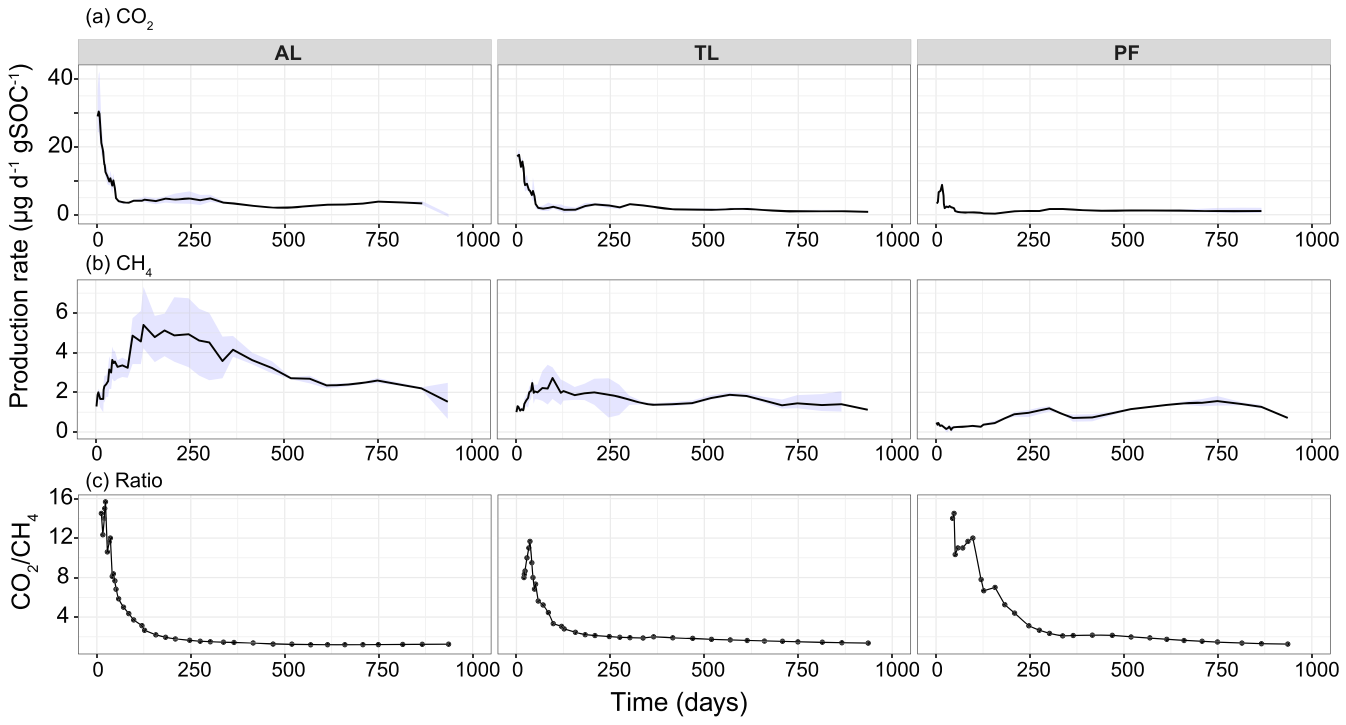

FIGURE 1 (a) CO_2 and (b) CH_4 production rates and (c) the ratio of CO_2 to CH_4 production rates over time for the active layer (AL), transition layer (TL), and permafrost (PF). The black line shows the average rate, and the blue shadow indicates the standard deviation of the replicates. The production rate was calculated based on the slope by a moving window using four measurements. The ratio of CO_2 to CH_4 was based on the average rate values of the CO_2 and CH_4 production rates. SOC, soil organic carbon [Colour figure can be viewed at wileyonlinelibrary.com]

characterized by higher moisture content (80.9%) and higher total C (17.7%) and total N (0.54%). Overall, C/N ratios were similar in all layers, and they ranged between 29.6 and 32.7%. Ferrous [Fe(II)] iron content in TL was approximately 10-fold higher than in AL and PF (37.5 vs. 3.7 and 3.9 mg L^{-1}, respectively). In contrast, Fe(III) contents were higher in AL and PF (11.8 and 8.9 mg L^{-1}) compared to TL (4.9 mg L^{-1}). The pH was slightly acidic for all samples and ranged from 5.4 in AL to 5.5 in TL and 5.6 in PF (Figure S2).

3.3 | Taxonomic and functional shifts on long-term warming

Long-term warming resulted in a pronounced shift in both the taxonomic and functional profiles of the microbial community in all layers (Figure 2). The taxonomic and functional profiles in TL and PF were more pronounced than those in AL. The strongest shift in the taxonomic profile was observed in PF, whereas the functional profile most strongly shifted in TL. A visual inspection based on a procrustes plot highlights lower concordance between the functional and taxonomic compositions for TL and PF than for AL (Figure S3). Regarding taxonomic shifts, the rpS3-based analysis confirmed the observed changes based on 16S rRNA, with some differences in the relative abundances of major microbial groups (Supplementary Document 1). In addition, the qPCR result revealed that the abundance of bacteria, and especially of methanogenic archaea overall, declined after long-term incubation (Figure S4).

3.3.1 | Taxonomic shifts within the bacterial community

The bacterial domain is dominated by members of Bacteroidetes, Firmicutes, and Proteobacteria, which comprise an average relative abundance of 53.7% (Figure 3). The long-term incubation resulted in an increase in the relative abundance of Bacteroidetes and Firmicutes in all layers but especially in TL (by 6.3 and 4.3%) and PF (by 10.9 and 2.3%). In addition, Patescibacteria were more abundant in the incubated samples (average 10.0%) compared to the original samples (average 5.1%). On the class level, strong increases on the incubation were observed for Parcubacteria, Microgenomatia, and Clostridia (Figure 4a). By contrast, long-term incubation resulted in a decrease in Proteobacteria and Actinobacteria during the long-term incubation (by 6.1 and 5.8%). Acidobacteria showed a low abundance in the original samples (3.0, 3.9, and 2.6% for AL, TL, and PF, respectively) and were negligible (below 0.01%) at the end of the incubation. A complete overview of the bacterial community changes at phylum level for all layers is provided in Table S2. On the class level, the strongest relative decreases were observed for Verrucomicrobiae, Alphaproteobacteria, Actinobacteria, and Acidobacteria (Figure 4a).

3.3.2 | Taxonomic shifts within the archaeal and fungal communities

The shift in the taxonomic profile is also reflected in the archaeal community structure on the phylum level (Figure 3) and on the family level shown as fold changes (Figure 4b). Pronounced fold changes were observed in Bathyarchaeia and Woesearchaeia, with overall increases of 7.0 and 11.4%, respectively, after long-term thaw exposure. A complete overview of the archaeal community changes at phylum level for all layers is provided in Table S3. The relative abundance of methanogenic archaea decreased after more than the 5-year warming scenario (average decrease of 40.8, 13.4, and 19.9% for AL, TL, and PF, respectively), but members related to the hydrogenotrophic Rice Cluster II lineage methanogens showed a clear, 18-fold increase in PF at the end of the incubation (1.2–21.8%). In addition, hydrogenotrophic Methanomicrobiales showed a substantial increase

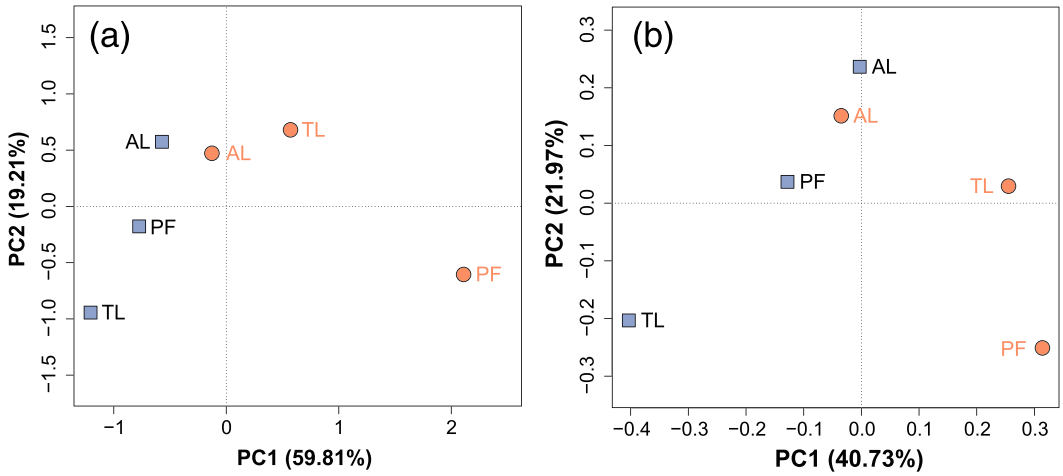

FIGURE 2 PCoA analysis on the (a) taxonomic profile and the (b) functional profile of the original (blue squares) and incubated (red circles) samples of the active layer (AL), transition layer (TL), and permafrost (PF). PC1 and PC2 indicate the first two principal coordinate axes. Percentages within parentheses indicate the variance explained by the respective PC axis [Colour figure can be viewed at wileyonlinelibrary.com]

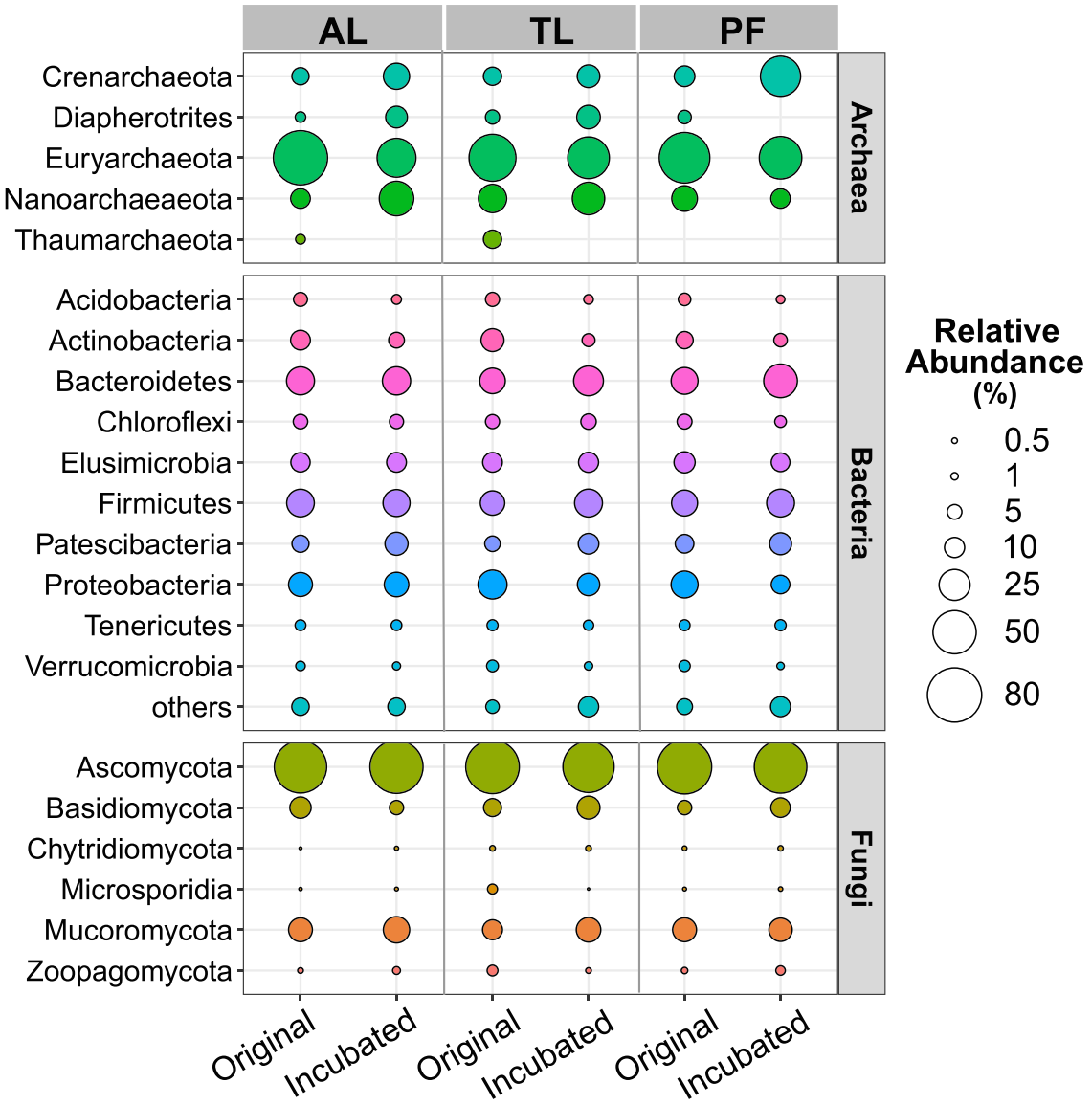

FIGURE 3 Taxonomic composition of the archaeal, bacterial, and fungal communities at phylum level for the active layer (AL), transition layer (TL), and permafrost (PF). The relative abundance was normalized by the total counts of each domain, respectively. For each layer, the two bars illustrate the original sample at the left and the incubated sample at the right. All lineages with relative abundance below 1% were grouped into "others" [Colour figure can be viewed at wileyonlinelibrary.com]

(9.1–24.5%) at least in TL, which is reflected in the fold increase in *Methanoregulaceae* (Figure 4b). The relative abundance of Methanosarcinales and Methanobacteriales declined in all layers. *Methanosarcinaceae*-specific sequences were detected only in the original AL, and the obligate acetoclastic *Methanosaetaceae* decreased in all samples on incubation.

The fungal community was dominated by members from Ascomycota (mean ± standard deviation, 73.7 ± 3.2%), Mucoromycota (13.8 ± 2.5%), and Basidiomycota (8.2 ± 3.4%) (Figure 3). The long-term incubation resulted in elevated abundance of fungal lineages such as *Glomerellaceae* (especially *Colletotrichum*), *Saccharomycetaceae* (*Sugiyamaella*), and *Ceratobasidiaceae* (*Ceratobasidium*) (Figure S5).

3.3.3 | Functional shifts

Overall, the functional profiles at metabolic pathway level showed similar responses and in most cases a decrease in long-term warming (Figure 5). The relative gene abundance for CH_4 cycling (CH_4 production and aerobic oxidation of CH_4) showed slight decreases. Similar patterns were also observed for carbon fixation, nitrogen, and sulfur cycling genes, despite the minor differences observed among the different layers.

To assess the functional changes in more detail, we analyzed the relative abundance changes for key functional marker genes (Table S4) of the major biogeochemical cycles (Figure 6). The analysis of individual key functional genes showed general agreement with the

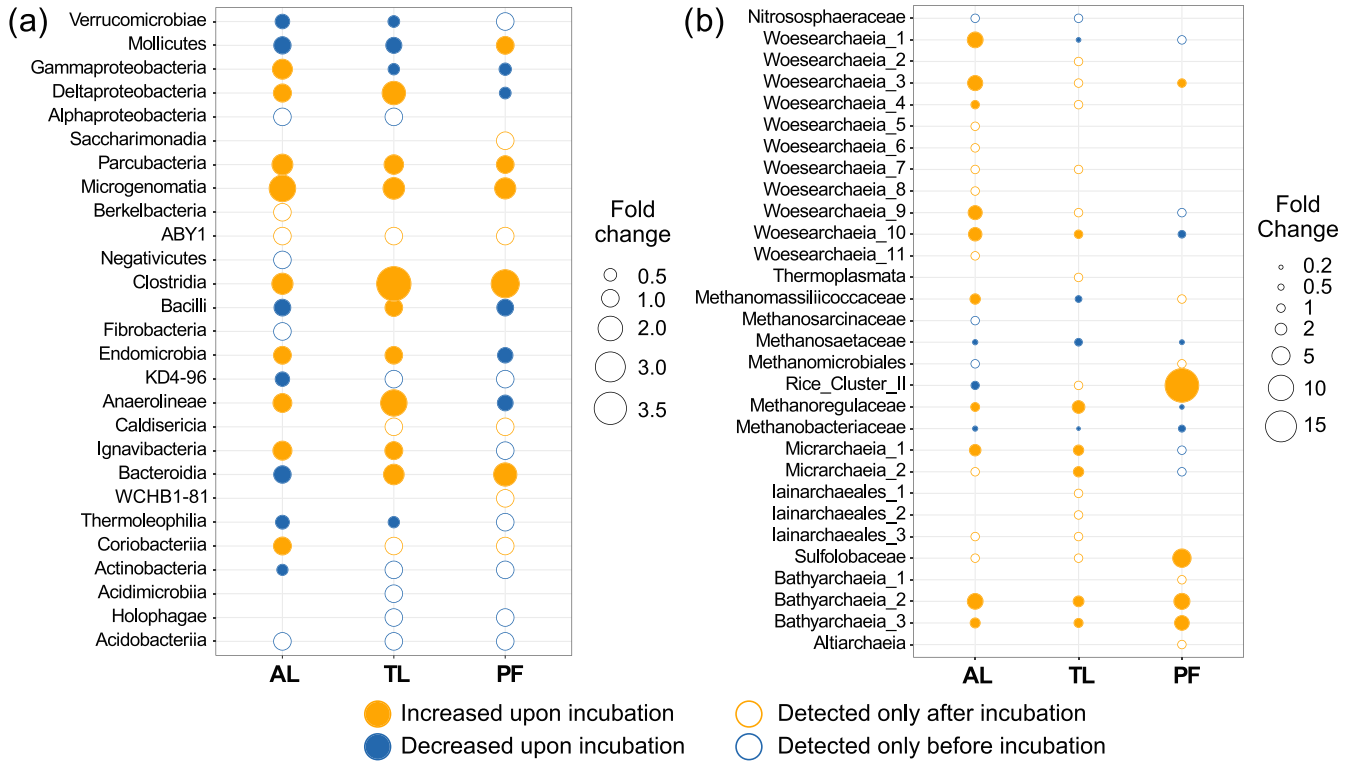

FIGURE 4 Fold changes of (a) bacteria at class level and (b) archaea at family level after long-term warming for the active layer (AL), transition layer (TL), and permafrost (PF). If an assignment to the class level was not available, the closest assignable taxonomic level from the SILVA132 database was used. Nondistinctive taxonomic labels were numbered for clarification. Orange dots indicate an increase; blue dots indicate a decrease after incubation. Nonfilled orange circles indicate a clade that was not detected in initial samples but present in incubated samples; blue circles indicate the lineage was present in the initial samples but not detected in incubated samples. Bubble sizes represent the fold changes after incubation. Bubble sizes of nonfilled circles do not represent fold changes. Note the different scales for the bacterial and archaeal plots [Colour figure can be viewed at wileyonlinelibrary.com]

analysis on whole pathway level as described earlier. Notwithstanding, permutation test did not show statistical significance ($p > 0.1$), and noticeable changes in some key gene abundance could be identified after long-term incubation for each layer. For acetogenesis (the Wood–Ljungdahl pathway), the change in acetyl-CoA synthase subunit gamma (*acsC*) in TL was most pronounced, but this was not reflected in the change observed for carbon monoxide dehydrogenase catalytic subunit (*cooS*). The *cooS* sequences were affiliated with Chloroflexi (35–61%), Proteobacteria (33–51%), and Actinobateria (2–22%). For methanogenesis, there was an overall decrease in relative abundance of the gene encoding for methyl-coenzyme M reductase subunit alpha (*mcrA*) in all layers, which matched with the shift in functional composition (Figure 5) and the overall decrease in methanogenic archaea that was observed in the 16S rRNA gene relative abundance (Figure 3).

Within the nitrogen cycle, different pathways showed distinct responses to long-term warming. Relative abundances of nitrate reduction genes (periplasmic nitrate reductase subunit alpha *napA* and nitrate reductase subunit alpha *narG*) increased in AL but decreased in TL and PF. Assimilatory nitrate reduction genes (assimilatory nitrate reductase catalytic subunit *nasA* and assimilatory nitrate reductase *narB*) show a general decrease. Denitrification and dissimilatory nitrate reduction to ammonium genes (iron-containing nitrite reductase *nrfA*, copper-containing nitrite reductase *nirK*, and nitrous oxide reductase *nosZ*) also show a general decrease in all samples. In contrast, nitric oxide reductase subunit beta (*norB*) shows an increase in all samples, with the strongest response in PF. The *norB*-gene carrier was primarily associated with Proteobacteria and Bacteroidetes, with increasing abundance of Bacteroidetes—in contrast to decreasing Proteobacteria—associated sequences after long-term warming (Figure S6). For nitrogen fixation, a decrease in nitrogenase reductase (*nifH*) was observed for AL, whereas an increase was observed for TL and PF. Nitrogen fixation was mainly associated with members of the Proteobacteria (>92% of hits).

Dissimilatory sulfate reduction genes (dissimilatory sulfite reductase *dsrAB*) decreased in AL and PF but increased in TL. Genes were affiliated with Proteobacteria (24–40%), Firmicutes (13–38%), and Acidobacteria (18–32%). Assimilatory sulfate reduction (phosphoadenosine phosphosulfate reductase *cysH*) showed minor decreases in AL and PF and the most pronounced decrease in TL.

Regarding carbohydrate metabolism, we focused on the protein groups related to cellulose and hemicellulose that are important for

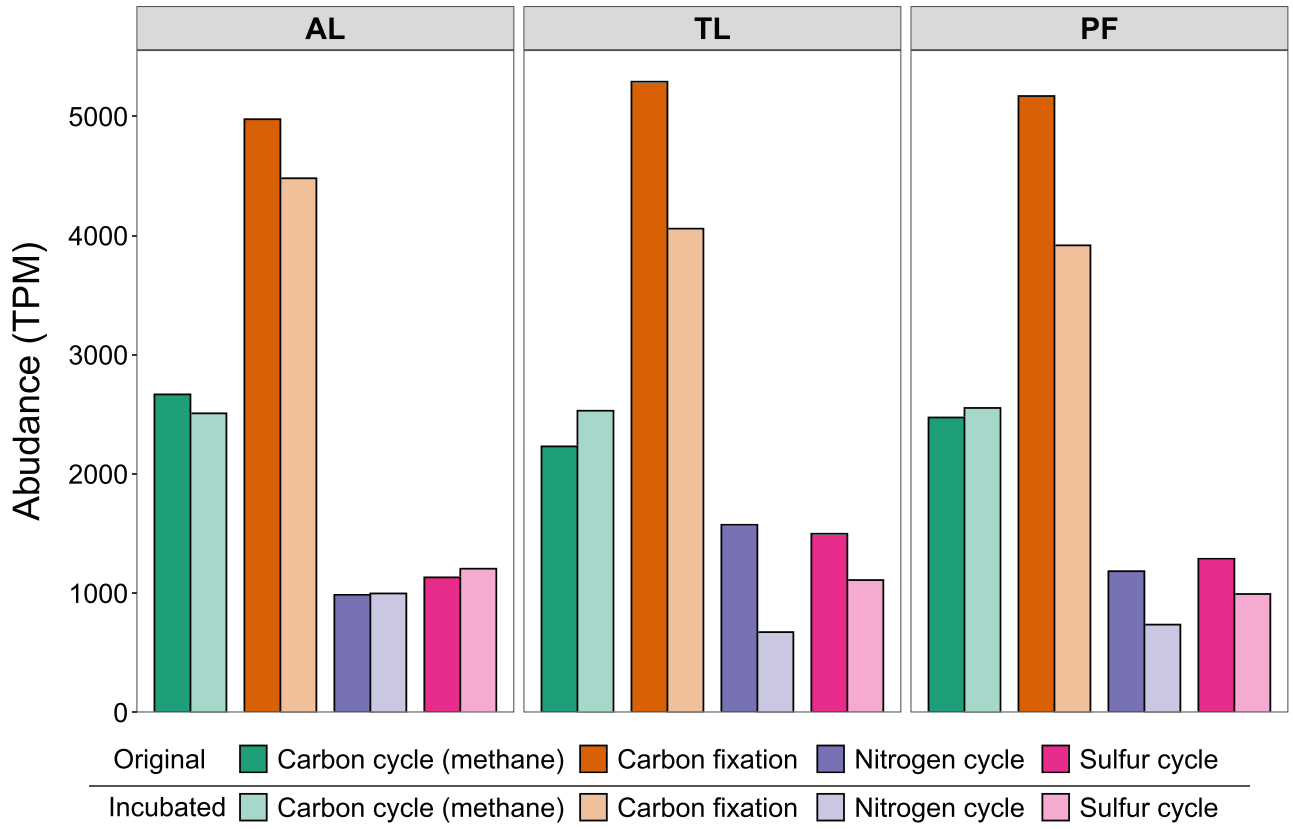

FIGURE 5 Shift in functional composition at pathway level over long-term incubation for the active layer (AL), transition layer (TL), and permafrost (PF). Carbon cycle (CH_4) includes both CH_4 production and aerobic CH_4 oxidation [Colour figure can be viewed at wileyonlinelibrary.com]

the decomposition of dead plant biomass (Figure 7; Figure S7). Like the aforementioned key genes, there are some notable changes despite the changes were not statistically significant ($p > 0.05$) by permutation. A general increase in abundance of cellulases (mainly GH5, GH9, GH3, and GH51) and hemicellulases (mainly GH31, GH43, and GH26) was observed after incubation. Moreover, a slight increase also occurred in carbohydrate binding modules (CBM, mainly CBM6 and CBM1) that bind cellulose or hemicellulose chains but lack catalytic activity. A further noticeable increase was observed in the lytic polysaccharide monooxygenases (mainly family AA10) and polysaccharide lyases (PLs), which are important enzymes involved in the deconstruction of cellulose and hemicellulose. Among the PLs that cleave uronic acid-containing polysaccharides, a clear increase was observed in PL11. The increases in enzymes pectate lyase (EC 4.2.2.2), exo-polygalacturonosidase (EC 3.2.1.82), and cellulase (EC3.2.1.4) were very pronounced in TL and PF and less in AL. The CAZy-encoding microorganisms primarily belonged to the Bacteroidetes (Table S5), and Bacteroidetes-associated CAZy classes showed substantial increases in all the layers (Figure S8). In addition, the enrichment of CAZy families within fungal functional guilds is associated with the decomposition of xyloglucan and xylan (GH54, CBM42, and GH31) across all layers, galactomannan (GH26) in the TL and PF, and cellulose (GH1, GH3, and GH5) in the AL (Figure S9).

4 | DISCUSSION

GHG production rates showed an immediate response in CO_2 release and a more steady response in CH_4 release over the 5-year incubation period. Therefore, initial CO_2 production rates largely outweighed CH_4 production rates. Rapid initial carbon degradation can result in high CO_2/CH_4 ratios,[62] which coincides with our observations. High initial CO_2 production was also observed in a 4-year incubation study on deep PF deposits from the Lena River delta, Siberia, whereas CH_4 production rates were much lower, which is consistent with our study.[63] An excess of CO_2 formation indicates fermentative processes as well as anaerobic respiration using alternative terminal electron acceptors, including NO_2^-/NO_3^-, Fe(III), and SO_4^{2-}, that are available in the sediment.[64] Indeed, Fe(III) and SO_4^{2-} were detected in the soil pore water of all layers before long-term incubation (Figure S2), whereas NO_3^- was not detected. Rapid initial activity is furthermore related to the presence of a considerable labile carbon pool in PF soils.[65,66] It has been reported that this labile organic matter is rapidly turned over under suitable conditions,[66,67] whereas the less-labile carbon was shown to fuel lower-rate CH_4 production in the long term.[7] A study on long-term carbon mineralization showed that under anoxic conditions only 25% of the aerobically released carbon was converted to CO_2 and CH_4.[63] The calibrated carbon degradation model executed

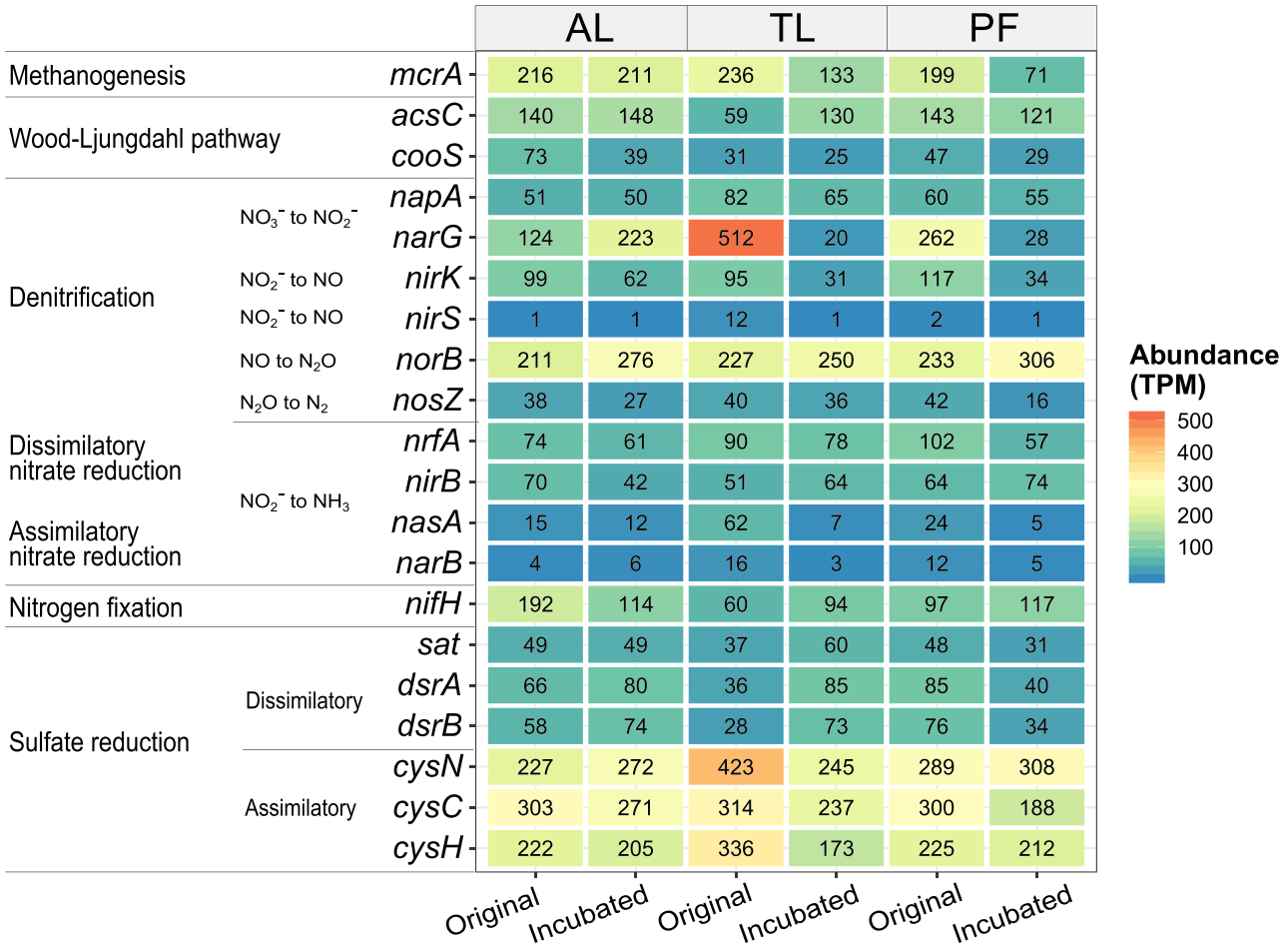

FIGURE 6 Heatmap of key genes involved in carbon, nitrogen, and sulfur cycling of anoxic ecosystems. The relative abundance is given in transcripts per kilobase million (TPM) for the active layer (AL), transition layer (TL), and permafrost (PF) [Colour figure can be viewed at wileyonlinelibrary.com]

in this study predicted 15.1% (aerobic) and 1.8% (anaerobic) initial carbon release over 100 years, highlighting the slow carbon release in the long term. This was mainly assigned to the presence of more stable complex organic compounds that are more inert and are therefore degrade much slowly.[38,68]

Increased water saturation coincides with ice-rich PF thaw, which stimulates wetland and thermokarst lake formation.[4] The gradual depletion of alternative terminal electron acceptors (e.g., NO_2^-/NO_3^-, Fe(III), and SO_4^{2-}) results in the formation of conditions suitable for methanogenesis.[38,69,70] In our study, the ratio of CO_2/CH_4 approached 1, and CH_4 production rate remained fairly constant after 300 days. This could indicate a depletion of alternative terminal electron acceptors. Similar observations were made by Knoblauch et al.,[6] where, in the long term, anoxic conditions also lead to stable though low rates of CH_4 production. Although methanogenesis became more important relative to CO_2 production, the abundance (both relative and absolute) of methanogenic archaea decreased, even though the relative abundance of hydrogenotrophic methanogens increased. This stresses the potential limitation of methanogenesis due to reduced substrate provision by fermentative microbial groups as well as a depletion of labile carbon. In our study, the first peak in CH_4 production could therefore be related with higher abundances of labile organic carbon that was present *in situ*. When labile organic matter pools get depleted, more stable organic matter fractions fuel the system. The slight increase in CH_4 production over time, especially in TL and PF, may indicate a shift toward the degradation of this less-labile organic matter pool. Evidence for this is provided by the functional microbial shifts using end-point metagenome analyses. Due to the higher structural complexity, the degradation of stabile organic molecules requires more energy, which results in higher temperature sensitivities compared to labile compounds.[71] The low GHG fluxes in the long term indicate that warming to 4°C still limits the turnover of more stable organic matter. Although the degradation of the less-labile organic matter fraction is much slower, it could still fuel a relatively stable methanogenic community.

In combination with the decreasing GHG production rates and a shift toward more methanogenic conditions, we observed substantial changes in microbial community structure and functions during the long-term warming scenario in all layers. The observed divergent shifts in community structure in the three different layers indicate

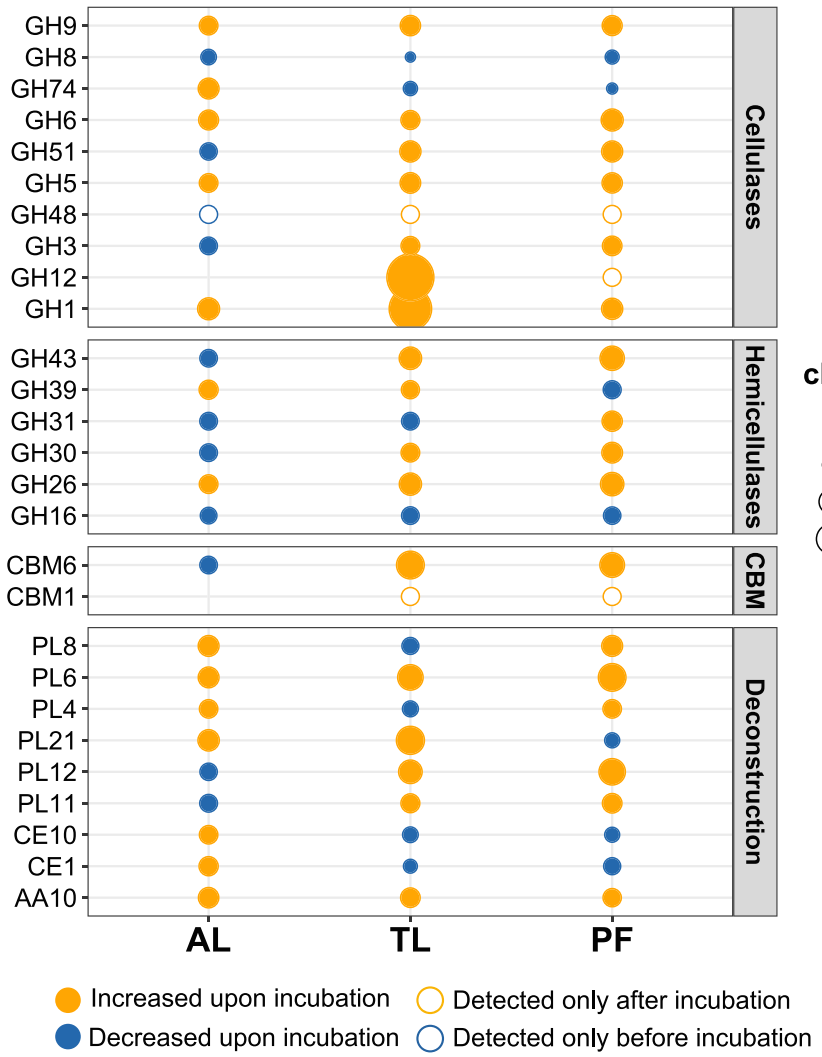

FIGURE 7 Fold changes in relative abundance (TPM [transcripts per kilobase million]) of the carbohydrate-active enzyme classes involved in the degradation of cellulose and hemicellulose in dead plant residuals detected in the active layer (AL), transition layer (TL), and permafrost (PF). Orange dots indicate an increase; blue dots indicate a decrease after incubation. Nonfilled orange circles indicate a clade that was not detected in initial samples but present in incubated samples; blue circles indicate that the lineage was present in the initial but absent in incubated samples. Bubble sizes represent the fold changes after long-term incubation. Bubble sizes of nonfilled circles do not represent fold changes. GH, glycoside hydrolases; GT, glycosyltransferases; PLs, polysaccharide lyases; CE, carbohydrate esterases; CBM, carbohydrate-binding modules; AA, auxiliary activities [Colour figure can be viewed at wileyonlinelibrary.com]

that PF thaw and long-term warming do not necessarily lead to the establishment of microbial communities more similar in taxonomic and functional composition. This is in contrast with previous observations by Mackelprang and coworkers, who studied PF metagenomes of AL and PF and observed a convergence of functional gene composition in a short term of 7 days.[20] The difference is potentially related to the differences in incubation time but also batch effects due to incubations in closed bottles, which prevent natural mixing with the surrounding soil matrix that may have contributed to this observation. This closed incubation on a lab scale could enable to approach the extreme potential of long-term old carbon degradation in PF; it should also be noted that this simplified setting inevitably eliminated the influence of other factors like vegetation cover and soil moisture, which was often observed by other studies.[18] Lab-scale incubations inevitably neglect the environmental complexity and interconnection between the profile under natural conditions and its role in modulating biodiversity and structure of the microbial community in situ. For example, in the closed system of lab incubations, progressive depletion of nutrients and electron acceptors gradually resulted in energetic stress for the microbial community, so that microbial activity was severely restricted although it did not cease. The anoxic setup also rejects the scenario of oxygen penetration into the soils, which was, however, beyond the focus of this study. Finally, the initial samples were preserved longer before DNA extraction than the incubation that could have manipulated the communities although this effect could be negligible as the cores were drilled when PF was entirely frozen and preserved in a continuously frozen state like natural PF.

Clostridia and Bacteroidia showed a positive response to thaw based on their relative abundances. These bacterial groups include many fermenting species that, for instance, play important roles in anaerobic fermentation of organic matter in anaerobic digestors.[72] Similar to our observations, Bacteroidetes were detected within the TL on a PF soil at Svalbard, Norway.[73] High occurrences of Bacteroidetes have been related with their metabolic flexibility, as well as rapid growth on easily accessible substrates.[74] Rapid growth on labile compounds could support their success on thaw, whereas their metabolic flexibility can support growth in the long term. Clostridia are fermentative bacteria that are generally well adapted to extreme conditions,[75] and they are able to ferment plant polysaccharides in soils.[76] Exposure to anoxic conditions led to an increase in relative

abundance of this lineage within PF-affected soils in the Lena delta[77] and High Arctic PF soil from Spitsbergen, Norway.[78] A study on Greenland PF-affected soils described a positive correlation of Clostridia with hydrolytic and oxidative enzyme activities.[79] These findings together with our observations suggest a potential role of Clostridia in the degradation of organic matter under thaw exposure and long-term warming. In addition, the dominance of and increase in Parcubacteria (Candidate Division OD1) and Microgenomatia (Candidate Division OP11) within the Patescibacteria superphylum[80] have been observed in PF thaw ponds[81,82] and PF-affected soils[83] similar to our observation. These taxa seem to be important players in a warming Arctic.

The long-term incubations also resulted in an overall decrease in abundance of methanogenic archaea, as briefly discussed earlier in the context of GHG production rates. This observation is in contrast with several short-term incubation studies on PF soils showing an increase in methanogen abundance.[15,20] The decrease in methanogens observed here is likely explained by the much-longer incubation period that resulted in an overall (relative) decrease in many genes and pathways involved in energy metabolisms and not just by gene- and gene-cluster-involved methanogenesis. Despite the overall decrease in methanogen abundance, an overall increase in members of the hydrogentrophic Rice Cluster II clade closely affiliated with Candidatus *Methanoflorens stordalenmirensis* was observed. This methanogenic archaeon is a key species in thawing PF[48] that can be used to predict CO_2 to CH_4 carbon emission ratios.[15,84] Simultaneously, *Methaonsarcinaceae* were detected only in AL before the incubation, and *Methanosaetaceae* decreased in all samples. Both families have been observed in PF peatlands and soils, and their existence is related to acetate availability.[14,85] Although this is in contrast with the study of Wei and coworkers[86] that showed a shift to Methanosarcinales after thaw exposure, it further supports the formation of a less acetate-driven system, which is related to the degradation of labile organic matter and the formation of a more hydrogen-driven system together with less-labile organic matter degradation.[87,88] Similar observations in long-term anoxic incubations were made earlier,[22] and also studies on ice-rich Yedoma deposits have suggested that acetate is a less-relevant substrate in PF deposits exposed to long-term anoxia.[64]

Unlike methanogenic archaea, Bathyarchaeia showed an overall increase in the course of the long-term warming scenario, whereas Thaumarchaeota were overall poorly abundant. The phylum of Bathyarchaeia represents an evolutionary diverse microbial group that is found in a wide range of organic-rich environments.[89] Interestingly, the recent discovery of the growth of Bathyarchaeota subgroup 8 (Bathy-8) on lignin suggests that it can play a key role in the degradation of less-labile plant organic matter fractions.[90] In addition, genomic and enzymatic analyses of several Bathyarchaeal lineages showed their capacity for acetogenesis and fermentation of a wide range of organic substrates, including cellulose and aromatic compounds.[91,92] Thaumarchaeota are related to aerobic NH_4 oxidation.[93] They are abundantly detected in environments with low ammonia concentrations, like PF, where they can provide an important role in the nitrogen cycle.[18,94,95]

In conjunction with the pronounced changes in GHG production potentials and microbial community structure, we observed large changes in the microbial metabolic potential. Overall, we observed a decrease in both methanogenic and carbon fixation genes, although the *acsC* gene encoding the gamma subunit of the CODH/ACS complex involved in the Wood–Ljungdahl pathway increases substantially in TL. The overall decrease in carbon cycling genes aligns with the decrease in GHG production rates that were observed after long-term incubation even though gene abundance cannot be directly related with GHG fluxes. Even if pairwise permutation test did not show statistical significance for three layers, the microbial community still showed adaptive change to a long-term energetically stressed condition although maintaining its functional potential for normal patterns of nutrient cycling. Microbial communities in the TL and PF that demonstrated more evident increment in CAZy-family genes have particularly environmental significance in feedback to climate.

Studies on PF soils have shown a lower abundance of nitrogen cycling genes for PF compared to the AL.[33,96] However, little is known about the functional response of the communities of the different layers on thaw. The study by Mackelprang and coworkers on PF from Hess Creek, Alaska, did observe rapid thaw responses for nitrogen and carbon cycle genes.[20] However, data on changes within these layers on long-term thaw exposure are lacking. In our study, nitrite and nitrate concentrations in the initial samples were negligible, and ammonium concentrations were highest in AL and lowest in PF. This data suggests that nitrogen supply potentially limits microbial growth and nitrogen supply is largely controlled by organic matter degradation and nitrogen fixation. After long-term incubation, gene abundances related to general nitrogen cycle processes decreased, whereas nitrogen fixation genes increased in TL and PF. Nitrogen fixation is an expensive process, which supports a general decrease in nitrogen fixation–associated genes when energy is limited or nitrogen supply is sufficient.[97] Our findings thus indicate that for TL and PF nitrogen availability can be a controlling factor and nitrogen demand may have increased during the incubations. Overall, nitrate reduction and denitrification gene abundances decreased, which supports a decrease in nitrate availability. Denitrification is mainly carried out by heterotrophic bacteria and requires organic carbon compounds as electron donors. The majority of canonical denitrifiers are facultative anaerobes.[97] Long-term anoxic incubation is therefore expected to result in a decrease in denitrifiers due to the depletion of alternative terminal electron acceptors, as was observed in this study. Within all layers an increase was observed in *norB*, which encodes for nitric oxide (NO) reductase subunit B and is involved in N_2O production.[98] It is further supported through initially high gene abundances of nitrate reduction and denitrification genes. Potential N_2O production is highly relevant in the context of climate feedbacks of thawing PF, as N_2O has a global warming potential of 298 over a time span of 100 years when including climate-carbon feedbacks.[2] Although there is no direct measurement of N_2O production in this study, N_2O production was shown to be enhanced in poorly drained thawing PF by previous studies.[99–102] Therefore, it is necessary to address the

question and to experimentally confirm whether N_2O emissions will increase under long-term anoxic thaw.

Little is known about microbial sulfur cycling in PF.[13] 16S rRNA gene and metagenomic sequences from sulfate-reducing microbes have been detected in several studies on PF.[32,103] Overall, an increase in dissimilatory sulfate reduction gene abundance was observed for AL and TL, whereas a decrease was observed for PF. For assimilatory sulfate reduction, a general decrease could be explained by an overall decreased availability of carbon, which suppresses growth. An overall decrease in sulfate reduction genes is obvious due to the expected depletion of sulfate under anoxic conditions. However, cryptic sulfur cycling that can be related to iron could supply oxidized sulfur species.[104] Overall, studies on sulfur cycling in PF indicate that changes in redox conditions after thaw stimulate sulfate reduction.[13] This is in line with a study on the effects of fire thaw that found that sulfate reduction genes were more abundant in anoxic deep soil layers.[27] However, in the long term it seems that dissimilatory sulfate reduction is mainly limited by sulfate availability, but experimental evidence is needed to support our observations.

The assumption that initial GHG fluxes and the short-term thaw response are associated with the labile organic matter pool whereas long-term GHG fluxes are controlled by the slower degradable organic matter pool agrees with the CAZy-based analysis. This analysis revealed a substantial increase in functional traits that are potentially involved in degrading cellulose and hemicellulose. This relates to scenarios in which the microbial community is able to adapt to anaerobic utilization of less-labile organic carbon from dead plant material after long-term thaw exposure of PF.[90,105] Similarly, an increased lignin decomposition contributed by Proteobacteria was revealed in AL soils of Arctic tundra soils after depleting soil labile C through a 975-day laboratory incubation.[106] As decomposition removes labile organic compounds, the remaining pools of soil carbon consist of a pool of less-labile or stable material, which will force the microbial community to acclimate. Through these microbial functional modulations, PF thaw and long-term exposure to warming result in steady GHG releases, even at low temperatures. Further temperature increases may increase GHG production rates given that less-degradable carbon is particularly sensitive to warming.[107] In addition to prokaryotes, fungi are generally resistant to warming and can play an important role in decomposing the less-labile or complex organic carbon.[108,109] The main fungal taxa in this study include many lineages able to degrade recalcitrant carbon (Figure S5). Following the fungal enzyme sets for plant polysaccharide degradation,[110] the enrichment of functional components involved in xyloglucan and xylan (GH54, CBM42, and GH31) across all layers underscores the importance of fungi in decomposing recalcitrant polysaccharides from plant residues at anoxic conditions. The increasing potential in degrading cellulose (GH1, GH3, and GH5) and galactomannan (GH26) within specific layers (Figure S9) likely implies different functional importance of fungi across layers. Future studies are therefore encouraged to include fungi to comprehensively understand the web of carbon degradation and spatial differentiation.

5 | CONCLUSIONS

This study used an anaerobic incubation system to investigate the potential of microbial response to environmental changes in which labile carbon is steadily depleted, and older carbon fractions are solely available in the long run. These conditions are specifically relevant to feed the boundary response potential of microbial communities into climate models. However, our setup excluded the contact to meltwater fluxes that carry gases and nutrients in field conditions. The three layers exhibited a general trend with an adaptation to the depletion of labile carbon and alternative terminal acceptors within approximately 1 year, despite the heterogeneity of the initial geochemistry of the three layers, and the significantly different CH_4 production potentials that were observed. This closed-off incubation system minimizes biases induced by other factors, including temperature, water table, and availability of nutrients. The system has imposed strong stress on the microbial population to favor lineages that can survive and function under alternative electron acceptor- and labile carbon-depleted conditions. The three different layers showed that PF thaw can lead to both taxonomic and functional adaptations for metabolizing less-labile carbon in the long term, which is unlikely to be caused by stochastic processes alone. This long-term microbial mechanism allows for relatively stable but low GHG production in long-term compared to short-term scenarios.

ACKNOWLEDGMENTS

This study was supported by the Helmholtz Gemeinschaft (HGF) through funding for S.L.'s Helmholtz Young Investigators Group (VH-NG-919). S.Y., C.K., S.L., J.W., and D.W. were supported by the German Ministry of Education and Research as part of the projects CarboPerm (grant numbers 03G0836A and 03G0836D) and KoPf (grant numbers 03F0764A and 03F0764F). S.Y. also acknowledges support from Chinese Academy of Sciences and National Key Research and Development Program of China (2020YFA0608501). We further acknowledge the financial support from the German Research Foundation (DFG) to C.K. through the Cluster of Excellence 'CLICCS', Universität Hamburg. T.L.V.B. and A.J.P. were supported by the Ministry of Culture and Science of North Rhine-Westphalia (Nachwuchsgruppe "Dr. Alexander Probst"). M.H.I.T.Z. and M.S.M.J. were supported by the Netherlands Organization for Scientific Research through the Netherlands Earth System Science Center (NESSC) Gravitation Grant (grant number 024.002.001 to M.H.I.T.Z. and M.S.M.J.), the Soehngen Institute of Anaerobic Microbiology (SIAM) Gravitation Grant (grant number 024.002.002 to M.S.M.J.), and the European Research Council Advanced Grant (grant number 339880 to M.S.M.J.). Dr. Jens Kallmayer and Jan Axel Kitte (GFZ German Research Centre for Geosciences) are acknowledged for their support in the lab.

DATA AVAILABILITY STATEMENT

The data that support the findings of this study are openly available in European Nucleotide Archive (ENA) at EMBL-EBI under acession number PRJEB38557 (https://www.ebi.ac.uk/ena/browser/view/PRJEB38557), sample accession number SAMEA6866753-SAMEA6866758.

ORCID

Sizhong Yang https://orcid.org/0000-0001-8417-593X
Susanne Liebner https://orcid.org/0000-0002-9389-7093
Josefine Walz https://orcid.org/0000-0002-0715-8738
Christian Knoblauch https://orcid.org/0000-0002-7147-1008
Till L. V. Bornemann https://orcid.org/0000-0003-3182-6596
Alexander J. Probst https://orcid.org/0000-0002-9392-6544
Dirk Wagner https://orcid.org/0000-0001-5064-497X
Mike S. M. Jetten https://orcid.org/0000-0002-4691-7039
Michiel H. in 't Zandt https://orcid.org/0000-0002-0497-4502

REFERENCES

1. Hugelius G, Strauss J, Zubrzycki S, et al. Estimated stocks of circumpolar permafrost carbon with quantified uncertainty ranges and identified data gaps. *Biogeosciences*. 2014;11(23):6573-6593.
2. IPCC. *Working Group I Contribution to the IPCC Fifth Assessment Report: Climate Change 2013: The Physical Science Basis, Summary for Policymakers*. IPCC, UN; 2013.
3. IPCC. *Climate Change 2007: The Physical Science Basis*. Cambridge, United Kingdom and New York, NY, USA; 2007.
4. Schuur EAG, McGuire AD, Schadel C, et al. Climate change and the permafrost carbon feedback. *Nature*. 2015;520(7546):171-179.
5. Dean JF, Middelburg JJ, Röckmann T, et al. Methane feedbacks to the global climate system in a warmer world. *Rev Geophys*. 2018;56(1):207-250.
6. Knoblauch C, Beer C, Liebner S, Grigoriev MN, Pfeiffer EM. Methane production as key to the greenhouse gas budget of thawing permafrost. *Nat Clim Chang*. 2018;8(4):309-312.
7. Douglas PMJ, Gonzalez Moguel R, Walter Anthony KM, et al. Clumped isotopes link older carbon substrates with slower rates of methanogenesis in northern lakes. *Geophys Res Lett*. 2020;47(6):e2019GL086756.
8. Pries CEH, Schuur EAG, Crummer KG. Thawing permafrost increases old soil and autotrophic respiration in tundra: Partitioning ecosystem respiration using $\delta^{13}C$ and $\delta^{14}C$. *Glob Chang Biol*. 2013;19(2):649-661.
9. Hayes DJ, Kicklighter DW, McGuire AD, et al. The impacts of recent permafrost thaw on land-atmosphere greenhouse gas exchange. *Environ Res Lett*. 2014;9(4):045005.
10. Schuur EAG, Bockheim J, Canadell JG, et al. Vulnerability of permafrost carbon to climate change: implications for the global carbon cycle. *Bioscience*. 2008;58(8):701-714.
11. Anthony KW, von Deimling TS, Nitze I, et al. 21st-century modeled permafrost carbon emissions accelerated by abrupt thaw beneath lakes. *Nat Commun*. 2018;9(1):3262.
12. Ping C, Jastrow J, Jorgenson M, Michaelson G, Shur Y. Permafrost soils and carbon cycling. *Soil*. 2015;1(1):147-171.
13. Mackelprang R, Saleska SR, Jacobsen CS, Jansson JK, Taş N. Permafrost meta-omics and climate change. *Annu Rev Earth Planet Sci*. 2016;44(1):439-462.
14. Ganzert L, Jurgens G, Munster U, Wagner D. Methanogenic communities in permafrost-affected soils of the Laptev Sea coast, Siberian Arctic, characterized by 16S rRNA gene fingerprints. *FEMS Microbiol Ecol*. 2007;59(2):476-488.
15. McCalley CK, Woodcroft BJ, Hodgkins SB, et al. Methane dynamics regulated by microbial community response to permafrost thaw. *Nature*. 2014;514(7523):478-481.
16. Schädel C, Schuur EAG, Bracho R, et al. Circumpolar assessment of permafrost C quality and its vulnerability over time using long-term incubation data. *Glob Chang Biol*. 2014;20(2):641-652.
17. Woodcroft BJ, Singleton CM, Boyd JA, et al. Genome-centric view of carbon processing in thawing permafrost. *Nature*. 2018;560(7716):49-54.
18. Jansson JK, Taş N. The microbial ecology of permafrost. *Nat Rev Microbiol*. 2014;12(6):414-425.
19. Hultman J, Waldrop MP, Mackelprang R, et al. Multi-omics of permafrost, active layer and thermokarst bog soil microbiomes. *Nature*. 2015;521(7551):208-212.
20. Mackelprang R, Waldrop MP, DeAngelis KM, et al. Metagenomic analysis of a permafrost microbial community reveals a rapid response to thaw. *Nature*. 2011;480(7377):368-371.
21. Rivkina E, Laurinavichius K, McGrath J, Tiedje J, Shcherbakova V, Gilichinsky D. Microbial life in permafrost. *Adv Space Res*. 2004;33(8):1215-1221.
22. Holm S, Walz J, Horn F, et al. Methanogenic response to long-term permafrost thaw is determined by paleoenvironment. *FEMS Microbiol Ecol*. 2020;96(3):fiaa021.
23. Mackelprang R, Burkert A, Haw M, et al. Microbial survival strategies in ancient permafrost: insights from metagenomics. *ISME J*. 2017;11(10):2305-2318.
24. Allan J, Ronholm J, Mykytczuk NC, Greer CW, Onstott TC, Whyte LG. Methanogen community composition and rates of methane consumption in Canadian High Arctic permafrost soils. *Environ Microbiol Rep*. 2014;6(2):136-144.
25. de Jong AEE, In 't Zandt MH, Meisel OH, et al. Increases in temperature and nutrient availability positively affect methane-cycling microorganisms in Arctic thermokarst lake sediments. *Environ Microbiol*. 2018;20(12):4314-4327.
26. Tveit AT, Urich T, Frenzel P, Svenning MM. Metabolic and trophic interactions modulate methane production by Arctic peat microbiota in response to warming. *Proc Natl Acad Sci*. 2015;112(19):E2507-E2516.
27. Taş N, Prestat E, McFarland JW, et al. Impact of fire on active layer and permafrost microbial communities and metagenomes in an upland Alaskan boreal forest. *ISME J*. 2014;8(9):1904-1919.
28. Singleton CM, McCalley CK, Woodcroft BJ, et al. Methanotrophy across a natural permafrost thaw environment. *ISME J*. 2018;12(10):2544-2558.
29. Bottos EM, Kennedy DW, Romero EB, et al. Dispersal limitation and thermodynamic constraints govern spatial structure of permafrost microbial communities. *FEMS Microbiol Ecol*. 2018;94(8):fiy110.
30. Taş N, Prestat E, Wang S, et al. Landscape topography structures the soil microbiome in arctic polygonal tundra. *Nat Commun*. 2018;9(1):1-13.
31. Liebner S, Harder J, Wagner D. Bacterial diversity and community structure in polygonal tundra soils from Samoylov Island, Lena Delta. *Int Microbiol*. 2008;11(3):195-202.
32. Steven B, Briggs G, McKay CP, Pollard WH, Greer CW, Whyte LG. Characterization of the microbial diversity in a permafrost sample from the Canadian high Arctic using culture-dependent and culture-independent methods. *FEMS Microbiol Ecol*. 2007;59(2):513-523.
33. Frank-Fahle BA, Yergeau E, Greer CW, Lantuit H, Wagner D. Microbial functional potential and community composition in permafrost-affected soils of the NW Canadian Arctic. *Plos One*. 2014;9(1):e84761.
34. Barbier BA, Dziduch I, Liebner S, et al. Methane-cycling communities in a permafrost-affected soil on Herschel Island, Western Canadian Arctic: active layer profiling of *mcrA* and *pmoA* genes. *FEMS Microbiol Ecol*. 2012;82(2):287-302.
35. Rivkina E, Petrovskaya L, Vishnivetskaya T, et al. Metagenomic analyses of the late Pleistocene permafrost - additional tools for reconstruction of environmental conditions. *Biogeosciences*. 2016;13(7):2207-2219.

36. Bischoff J, Mangelsdorf K, Gattinger A, et al. Response of methanogenic archaea to Late Pleistocene and Holocene climate changes in the Siberian Arctic. *Global Biogeochem Cycles*. 2013;27(2):305-317.
37. Elberling B, Michelsen A, Schädel C, et al. Long-term CO_2 production following permafrost thaw. *Nat Clim Chang*. 2013;3(10):890-894.
38. Lee H, Schuur EAG, Inglett KS, Lavoie M, Chanton JP. The rate of permafrost carbon release under aerobic and anaerobic conditions and its potential effects on climate. *Glob Chang Biol*. 2012;18(2):515-527.
39. Bracho R, Natali S, Pegoraro E, et al. Temperature sensitivity of organic matter decomposition of permafrost-region soils during laboratory incubations. *Soil Biol Biochem*. 2016;97:1-14.
40. Hermoso de Mendoza I, Beltrami H, MacDougall, Mareschal JC. Lower boundary conditions in land surface models – effects on the permafrost and the carbon pools: a case study with CLM4.5. *Geosci Model Dev*. 2020;13(3):1663-1683.
41. Estop-Aragones C, Olefeldt D, Abbott BW, et al. Assessing the potential for mobilization of old soil carbon after permafrost thaw: A synthesis of ^{14}C measurements from the northern permafrost region. *Global Biogeochem Cycles*. 2020;34(9):e2020GB006672.
42. Boike J, Kattenstroth B, Abramova K, et al. Baseline characteristics of climate, permafrost and land cover from a new permafrost observatory in the Lena River Delta, Siberia (1998-2011). *Biogeosciences*. 2013;10(3):2105-2128.
43. Schwamborn G, Rachold V, Grigoriev MN. Late Quaternary sedimentation history of the Lena Delta. *Quat Int*. 2002;89(1):119-134.
44. Kutzbach L, Wagner D, Pfeiffer E-M. Effect of microrelief and vegetation on methane emission from wet polygonal tundra, Lena Delta, Northern Siberia. *Biogeochemistry*. 2004;69(3):341-362.
45. Walz J, Knoblauch C, Bohme L, Pfeiffer EM. Regulation of soil organic matter decomposition in permafrost-affected Siberian tundra soils - Impact of oxygen availability, freezing and thawing, temperature, and labile organic matter. *Soil Biol Biochem*. 2017;110:34-43.
46. Liebner S, Zeyer J, Wagner D, Schubert C, Pfeiffer E-M, Knoblauch C. Methane oxidation associated with submerged brown mosses reduces methane emissions from Siberian polygonal tundra. *J Ecol*. 2011;99(4):914-922.
47. Viollier E, Inglett PW, Hunter K, Roychoudhury AN, Van Cappellen P. The ferrozine method revisited: Fe (II)/Fe (III) determination in natural waters. *Appl Geochem*. 2000;15(6):785-790.
48. Liebner S, Ganzert L, Kiss A, Yang S, Wagner D, Svenning MM. Shifts in methanogenic community composition and methane fluxes along the degradation of discontinuous permafrost. *Front Microbiol*. 2015;6:356.
49. Kieser S, Brown J, Zdobnov EM, Trajkovski M, McCue LA. ATLAS: a Snakemake workflow for assembly, annotation, and genomic binning of metagenome sequence data. *BMC Bioinf*. 2019;21:257.
50. Hyatt D, Chen G-L, LoCascio PF, Land ML, Larimer FW, Hauser LJ. Prodigal: prokaryotic gene recognition and translation initiation site identification. *BMC Bioinf*. 2010;11(1):119.
51. Huerta-Cepas J, Forslund K, Coelho LP, et al. Fast genome-wide functional annotation through orthology assignment by eggNOG-Mapper. *Mol Biol Evol*. 2017;34(8):2115-2122.
52. Buchfink B, Xie C, Huson DH. Fast and sensitive protein alignment using DIAMOND. *Nat Methods*. 2015;12(1):59-60.
53. Suzek BE, Wang Y, Huang H, McGarvey PB, Wu CH, UniProt Consortium. UniRef clusters: a comprehensive and scalable alternative for improving sequence similarity searches. *Bioinformatics*. 2014;31(6):926-932.
54. Huerta-Cepas J, Szklarczyk D, Heller D, et al. eggNOG 5.0: a hierarchical, functionally and phylogenetically annotated orthology resource based on 5090 organisms and 2502 viruses. *Nucleic Acids Res*. 2018;47(D1):D309-D314.
55. Quast C, Pruesse E, Yilmaz P, et al. The SILVA ribosomal RNA gene database project: improved data processing and web-based tools. *Nucleic Acids Res*. 2013;41(D1):D590-D596.
56. Camacho C, Coulouris G, Avagyan V, et al. BLAST+: architecture and applications. *BMC Bioinf*. 2009;10(1):421.
57. Hug LA, Baker BJ, Anantharaman K, et al. A new view of the tree of life. *Nat Microbiol*. 2016;1(5):16048.
58. *R Core Team: A language and environment for statistical computing. R Foundation for Statistical Computing*. Vienna, Austria.
59. Yang S. otuSummary: Summarizing OTU table regarding the composition, abundance and beta diversity of abundant and rare biospheres. R package version 0.1.0. https://github.com/cam315/otuSummary. 2020.
60. Oksanen J, Blanchet FG & Friendly M et al. vegan: Community Ecology Package. R package version 2.5–6. https://CRAN.R-project.org/package=vegan. 2019.
61. Wickham H. *ggplot2: Elegant Graphics for Data Analysis*. New York: Springer-Verlag; 2016.
62. Gao C, Sander M, Agethen S, Knorr K-H. Electron accepting capacity of dissolved and particulate organic matter control CO_2 and CH_4 formation in peat soils. *Geochim Cosmochim Acta*. 2019;245:266-277.
63. Knoblauch C, Beer C, Sosnin A, Wagner D, Pfeiffer E-M. Predicting long-term carbon mineralization and trace gas production from thawing permafrost of Northeast Siberia. *Glob Chang Biol*. 2013;19(4):1160-1172.
64. Ewing SA, O'Donnell JA, Aiken GR, et al. Long-term anoxia and release of ancient, labile carbon upon thaw of Pleistocene permafrost. *Geophys Res Lett*. 2015;42(24):10730-10738.
65. Mueller CW, Rethemeyer J, Kao-Kniffin J, Löppmann S, Hinkel KM, Bockheim GJ. Large amounts of labile organic carbon in permafrost soils of northern Alaska. *Glob Chang Biol*. 2015;21(7):2804-2817.
66. Rodionow A, Flessa H, Kazansky O, Guggenberger G. Organic matter composition and potential trace gas production of permafrost soils in the forest tundra in northern Siberia. *Geoderma*. 2006;135:49-62.
67. Strauss J, Schirrmeister L, Grosse G, et al. The deep permafrost carbon pool of the Yedoma region in Siberia and Alaska. *Geophys Res Lett*. 2013;40(23):6165-6170.
68. Dutta K, Schuur EAG, Neff JC, Zimov SA. Potential carbon release from permafrost soils of Northeastern Siberia. *Glob Chang Biol*. 2006;12(12):2336-2351.
69. Wagner D. Effect of varying soil water potentials on methanogenesis in aerated marshland soils. *Sci Rep*. 2017;7(1):14706.
70. Enzmann F, Mayer F, Rother M, Holtmann D. Methanogens: biochemical background and biotechnological applications. *AMB Express*. 2018;8(1):1-1.
71. Fierer N, Craine JM, McLauchlan K, Schimel JP. Litter quality and the temperature sensitivity of decomposition. *Ecology*. 2005;86(2):320-326.
72. Goud RK, Raghavulu SV, Mohanakrishna G, Naresh K, Mohan SV. Predominance of Bacilli and Clostridia in microbial community of biohydrogen producing biofilm sustained under diverse acidogenic operating conditions. *Int J Hydrogen Energy*. 2012;37(5):4068-4076.
73. Müller O, Bang-Andreasen T, White RA, et al. Disentangling the complexity of permafrost soil by using high resolution profiling of microbial community composition, key functions and respiration rates. *Environ Microbiol*. 2018;20(12):4328-4342.
74. Fierer N, Bradford MA, Jackson RB. Toward an ecological classification of soil bacteria. *Ecology*. 2007;88(6):1354-1364.
75. Chades T, Scully SM, Ingvadottir EM, Orlygsson J. Fermentation of mannitol extracts from brown macro algae by thermophilic *Clostridia*. *Front Microbiol*. 2018;9:1931.
76. Boutard M, Cerisy T, Nogue PY, et al. Functional diversity of carbohydrate-active enzymes enabling a bacterium to ferment plant biomass. *PLoS Genet*. 2014;10(11):e1004773.

77. Wagner D, Kobabe S, Liebner S. Bacterial community structure and carbon turnover in permafrost-affected soils of the Lena Delta, northeastern Siberia. *Can J Microbiol*. 2009;55(1):73-83.
78. Hansen AA, Herbert RA, Mikkelsen K, et al. Viability, diversity and composition of the bacterial community in a high Arctic permafrost soil from Spitsbergen, Northern Norway. *Environ Microbiol*. 2007; 9(11):2870-2884.
79. Gittel A, Barta J, Kohoutova I, et al. Site- and horizon-specific patterns of microbial community structure and enzyme activities in permafrost-affected soils of Greenland. *Front Microbiol*. 2014;5:541.
80. Rinke C, Schwientek P, Sczyrba A, et al. Insights into the phylogeny and coding potential of microbial dark matter. *Nature*. 2013; 499(7459):431-437.
81. Wurzbacher C, Nilsson RH, Rautio M, Peura S. Poorly known microbial taxa dominate the microbiome of permafrost thaw ponds. *ISME J*. 2017;11(8):1938-1941.
82. Vigneron A, Cruaud P, Pignet P, et al. Archaeal and anaerobic methane oxidizer communities in the Sonora Margin cold seeps, Guaymas Basin (Gulf of California). *ISME J*. 2013;7(8):1595-1608.
83. Frey B, Rime T, Phillips M, et al. Microbial diversity in European alpine permafrost and active layers. *FEMS Microbiol Ecol*. 2016;92(3): fiw018.
84. Mondav R, Woodcroft BJ, Kim E-H, et al. Discovery of a novel methanogen prevalent in thawing permafrost. *Nat Commun*. 2014;5(1): 3212.
85. Yavitt JB, Seidmann-Zager M. Methanogenic conditions in northern peat soils. *Geomicrobiol J*. 2006;23(2):119-127.
86. Wei SP, Cui HP, Zhu YH, et al. Shifts of methanogenic communities in response to permafrost thaw results in rising methane emissions and soil property changes. *Extremophiles*. 2018;22(3):447-459.
87. Yang S, Liebner S, Winkel M, et al. In-depth analysis of core methanogenic communities from high elevation permafrost-affected wetlands. *Soil Biol Biochem*. 2017;111:66-77.
88. Buitrón G, Kumar G, Martinez-Arce A, Moreno G. Hydrogen and methane production via a two-stage processes (H_2-SBR + CH_4-UASB) using tequila vinasses. *Int J Hydrogen Energy*. 2014;39(33): 19249-19255.
89. Evans PN, Parks DH, Chadwick GL, et al. Methane metabolism in the archaeal phylum Bathyarchaeota revealed by genome-centric metagenomics. *Science*. 2015;350(6259):434-438.
90. Yu T, Wu W, Liang W, Lever MA, Hinrichs K-U, Wang F. Growth of sedimentary Bathyarchaeota on lignin as an energy source. *Proc Natl Acad Sci*. 2018;115(23):6022-6027.
91. He Y, Li M, Perumal V, et al. Genomic and enzymatic evidence for acetogenesis among multiple lineages of the archaeal phylum Bathyarchaeota widespread in marine sediments. *Nat Microbiol*. 2016; 1(6):16035.
92. Lazar CS, Baker BJ, Seitz K, et al. Genomic evidence for distinct carbon substrate preferences and ecological niches of Bathyarchaeota in estuarine sediments. *Environ Microbiol*. 2016;18(4):1200-1211.
93. Kits KD, Sedlacek CJ, Lebedeva EV, et al. Kinetic analysis of a complete nitrifier reveals an oligotrophic lifestyle. *Nature*. 2017; 549(7671):269-272.
94. Auguet J-C, Casamayor EO. Partitioning of Thaumarchaeota populations along environmental gradients in high mountain lakes. *FEMS Microbiol Ecol*. 2013;84(1):154-164.
95. Pester M, Schleper C, Wagner M. The Thaumarchaeota: an emerging view of their phylogeny and ecophysiology. *Curr Opin Microbiol*. 2011;14(3):300-306.
96. Yergeau E, Hogues H, Whyte LG, Greer CW. The functional potential of high Arctic permafrost revealed by metagenomic sequencing, qPCR and microarray analyses. *ISME J*. 2010;4(9):1206-1214.
97. Kuypers MMM, Marchant HK, Kartal B. The microbial nitrogen-cycling network. *Nat Rev Microbiol*. 2018;16(5):263-276.
98. Suzuki M, Arai H, Ishii M, Igarashi Y. Gene structure and expression profile of cytochrome bc nitric oxide reductase from *Hydrogenobacter thermophilus* TK-6. *Biosci Biotechnol Biochem*. 2006; 70(7):1666-1671.
99. Elberling B, Christiansen HH, Hansen BU. High nitrous oxide production from thawing permafrost. *Nat Geosci*. 2010;3(5):332-335.
100. Abbott BW, Jones JB. Permafrost collapse alters soil carbon stocks, respiration, CH_4, and N_2O in upland tundra. *Glob Chang Biol*. 2015; 21(12):4570-4587.
101. Marushchak ME, Pitkamaki A, Koponen H, Biasi C, Seppala M, Martikainen PJ. Hot spots for nitrous oxide emissions found in different types of permafrost peatlands. *Glob Chang Biol*. 2011;17(8): 2601-2614.
102. Voigt C, Marushchak ME, Lamprecht RE, et al. Increased nitrous oxide emissions from Arctic peatlands after permafrost thaw. *Proc Natl Acad Sci*. 2017;114(24):6238-6243.
103. Lipson DA, Haggerty JM, Srinivas A, Raab TK, Sathe S, Dinsdale EA. Metagenomic insights into anaerobic metabolism along an arctic peat soil profile. *Plos One*. 2013;8(5):e64659.
104. Holmkvist L, Ferdelman TG, Jørgensen BB. A cryptic sulfur cycle driven by iron in the methane zone of marine sediment (Aarhus Bay, Denmark). *Geochim Cosmochim Acta*. 2011;75(12):3581-3599.
105. Mayumi D, Mochimaru H, Tamaki H, et al. Methane production from coal by a single methanogen. *Science*. 2016;354(6309):222-225.
106. Tao X, Feng J, Yang Y, et al. Winter warming in Alaska accelerates lignin decomposition contributed by Proteobacteria. *Microbiome*. 2020;8(1):84.
107. Davidson EA, Janssens IA. Temperature sensitivity of soil carbon decomposition and feedbacks to climate change. *Nature*. 2006; 440(7081):165-173.
108. Newsham KK, Garnett MH, Robinson CH, Cox F. Discrete taxa of saprotrophic fungi respire different ages of carbon from Antarctic soils. *Sci Rep*. 2018;8(1):7866.
109. Luláková P, Perez-Mon C, Šantrůčková H, Ruethi J, Frey B. High-alpine permafrost and active-layer soil microbiomes differ in their response to elevated temperatures. *Front Microbiol*. 2019;10:668.
110. van den Brink J, de Vries RP. Fungal enzyme sets for plant polysaccharide degradation. *Appl Microbiol Biotechnol*. 2011;91(6): 1477-1492.

SUPPORTING INFORMATION

Additional supporting information may be found in the online version of the article at the publisher's website.

How to cite this article: Yang S, Liebner S, Walz J, et al. Effects of a long-term anoxic warming scenario on microbial community structure and functional potential of permafrost-affected soil. *Permafrost and Periglac Process*. 2021;32(4): 641-656. doi:10.1002/ppp.2131